Roles of phosphorylation of myosin binding protein-C and troponin I in mouse cardiac muscle twitch dynamics

Carl W. Tong, Robert D. Gaffin, David C. Zawieja and Mariappan Muthuchamy

336 Reynolds Medical Building, Cardiovascular Research Institute and Department of Medical Physiology, College of Medicine, Texas A & M University System Health Science Center, College Station, TX 77843-1114, USA

A normal heart increases its contractile force with increasing heart rate. Although calcium handling and myofibrillar proteins have been implicated in maintaining this positive force–frequency relationship (FFR), the exact mechanisms by which it occurs have not been addressed. In this study, we have developed an analytical method to define the calcium–force loop data, which characterizes the function of the contractile proteins in response to calcium that is independent of the calcium handling proteins. Results demonstrate that increasing the stimulation frequency causes increased force production per unit calcium concentration and decreased frequency-dependent calcium sensitivity during the relaxation phase. We hypothesize that phosphorylation of myosin binding protein-C (MyBP-C) and troponin I (TnI) acts coordinately to change the rates of force generation and relaxation, respectively. To test this hypothesis, we performed simultaneous calcium and force measurements on stimulated intact mouse papillary bundles before and after inhibition of MyBP-C and TnI phosphorylation using the calcium/calmodulin kinase II (CaMK2) inhibitor autocamtide-2 related inhibitory peptide, or the protein kinase A (PKA) inhibitor 14–22 amide. CaMK2 inhibition reduced both MyBP-C and TnI phosphorylation and decreased active force without changing the magnitude of the $[Ca^{2+}]_i$ transient. This reduced the normalized change in force per change in calcium by 19–39%. Data analyses demonstrated that CaMK2 inhibition changed the myofilament characteristics via a crossbridge feedback mechanism. These results strongly suggest that the phosphorylation of MyBP-C and TnI contributes significantly to the rates of force development and relaxation.

(Resubmitted 6 February 2004; accepted after revision 7 June 2004; first published online 11 June 2004)
Corresponding author M. Muthuchamy: 336 Reynolds Medical Building, Cardiovascular Research Institute and Department of Medical Physiology, College of Medicine, Texas A & M University System Health Science Center, College Station, TX 77843-1114, USA. Email: marim@tamu.edu

A normal heart shows a positive force–frequency relationship (FFR) (Braunwald *et al.* 2001) in which the strength of cardiac contraction increases as heart rate increases. This positive FFR is lost in heart failure (Braunwald *et al.* 2001). Historically, the FFR response can be explained by increased basal intracellular calcium concentrations overwhelming the sarcoplasmic reticulum ATPase (SERCA2a). In recent studies, the calcium handling proteins SERCA2a (Alpert *et al.* 1998; Hashimoto *et al.* 2000; Heerdt *et al.* 2000; Miyamoto *et al.* 2000; Munch *et al.* 2000), phospholamban (Bluhm *et al.* 2000; Hagemann *et al.* 2000), and the sarcolemmal L-type calcium channel (LTCC) (Lemaire *et al.* 1998) have shown frequency-dependent characteristics that contribute to a positive FFR. In addition to the effects of these calcium handling proteins, experimental evidence suggests that the myofilaments may also change their function in a frequency-dependent manner to support a positive FFR. Evidence supporting this includes the following: (1) SERCA2a overexpression rescue of a rat heart failure model still required an increased pre-load (Miyamoto *et al.* 2000); (2) matching inward calcium influx with sarcoplasmic reticulum (SR) calcium concentration did not improve performance of myocytes that had been treated with the calcium/calmodulin kinase II (CaMK2) inhibitor KN-93 (Li *et al.* 1997); and (3) the calcium sensitizer agent levosimendan restored the positive FFR of muscle strips from end stage heart failure patients without changing the intracellular calcium concentration ($[Ca^{2+}]_i$) (Brixius *et al.* 2002). Furthermore, mutations in sarcomeric proteins can cause dilated cardiomyopathy (DCM) (Towbin & Bowles, 2002) and hypertrophic

 DOI: 10.1113/jphysiol.2004.062539

cardiomyopathy (HCM) (Spirito *et al.* 1997; Bonne *et al.* 1998). Although the above studies suggest possible roles for the myofilament proteins in modulating the positive FFR, the mechanisms by which this occurs have not been determined.

A previous study that analysed $[Ca^{2+}]_i$ and force measurements in mouse cardiac trabeculae suggested a frequency-dependent sensitization of the myofilaments (Gao *et al.* 1998). To further define the roles of myofilament proteins in the positive FFR, we have developed an analytical method that allows dissection of myofilament function in the milieu of $[Ca^{2+}]_i$ transients. In the context of a positive FFR, the forward and reverse transitions must take place quickly enough to allow the changing rates of crossbridge attachment and detachment to provide the overall net effects of force generation and relaxation. Several studies have shown that PKA-dependent phosphorylation of myofilament proteins, specifically troponin I (TnI) and myosin binding protein-C (MyBP-C), play an imperative role in modulating this crossbridge cycling (Strang *et al.* 1994; Solaro & Rarick, 1998; Winegrad, 1999).

MyBP-C, a component of the thick filament of striated muscle (Offer *et al.* 1973), is located in seven to nine bands within the C region of the sarcomere that are spaced 43 nm apart (Craig & Offer, 1976). Cardiac MyBP-C has three sites that can be phosphorylated by a combination of CaMK2 and protein kinase A (PKA) (Gautel *et al.* 1995). CaMK2 phosphorylation of MyBP-C appears to enable the two PKA sites on MyBP-C to be phosphorylated (Gautel *et al.* 1995; McClellan *et al.* 2001). It has been suggested that phosphorylated MyBP-C may change crossbridge interaction dynamics by (1) loosening the packing of myosin thereby increasing the thick filament diameter with the net result of decreasing the myosin head to actin distance (Weisberg & Winegrad, 1996; Winegrad, 1999, 2000), and/or (2) preventing MyBP-C from binding to the myosin–S2 domain to allow greater crossbridge flexibility (Gruen & Gautel, 1999; Gruen *et al.* 1999; Kunst *et al.* 2000). Extraction of MyBP-C in skinned fibre studies also shows a decrease in the cooperativity of myofilament activation (Hofmann *et al.* 1991). McClellan *et al.* (2001) have recently shown that calcium-mediated phosphorylation of MyBP-C correlates well with increases in maximum force. Thus, ample evidence exists to suggest that phosphorylation of MyBP-C changes myofilament function.

In order to balance the increase in force associated with the FFR, the sarcomeres need a mechanism that increases the rate of relaxation. Phosphorylation of TnI decreases the calcium sensitivity of myofilaments (Solaro *et al.* 1976; Solaro & Rarick, 1998) suggesting that phosphorylated TnI promotes relaxation. Recent kinetic studies clearly show that PKA phosphorylation of TnI increases the rate of relaxation (Zhang *et al.* 1995; Kentish *et al.* 2001). Hence, we hypothesize that the phosphorylation of MyBP-C and TnI acts coordinately to change the rates of force generation and relaxation, respectively, and thus influence the resultant FFR of cardiac muscle.

To investigate the above premise, we performed simultaneous force and $[Ca^{2+}]_i$ measurements in intact papillary muscle bundles from mice hearts at increasing stimulation frequencies under control and CaMK2 inhibited conditions. We then analysed the calcium–force loop at specific points and at three different segments of the contraction cycle to examine myofilament function. Our results show that increasing stimulation frequency increased force production per unit change of calcium concentration and decreased frequency-dependent calcium sensitivity of the myofilaments during the relaxation phase. Furthermore, the data provide the first evidence that phosphorylation of MyBP-C and TnI affects the dynamics of crossbridge kinetics and the resultant FFR.

Methods

Force–frequency measurements at 34°C

All experiments using mouse hearts were approved by the Texas A & M University Animal Care Committee. Mice (FVB/N strain; 3–4 months old) were anaesthetized with sodium pentobarbital (60 mg (kg body weight)$^{-1}$, I.P.) and hearts quickly excised and placed in a Krebs–Henseleit (KH) solution containing 30 mM of 2,3-butadione monoxime (BDM; Sigma, USA) at 4°C. The KH solution consisted of 119.0 mM NaCl, 11.0 mM glucose, 4.6 mM KCl, 25.0 mM $NaHCO_3$, 1.2 mM KH_2PO_4, 1.2 mM $MgSO_4$, and 1.8 mM $CaCl_2$. The KH solution was equilibrated with 95% O_2 and 5% CO_2. Thin uniform papillary muscle bundles were carefully dissected from right ventricle. The papillary muscle approximates a circular (eclipse) cone as it tapers from the right ventricular wall towards the tricuspid valve with the width of the base (d_w) being 0.345–0.518 mm, the width where the chordae tendinae (d_c) attaches 0.115–0.155 mm, and the length 1–2 mm. The depth at the base of the fibres is usually 0.2–0.25 mm, which is within the limitation of the maximum diffusion distance of 0.2 mm (radius). An equivalent radius (r_{eq}) of the muscle is found by equating the volume of the circular cone to the volume of a cylindrical cone of the same length, which is calculated by the following equation:

$$r_{\mathrm{eq}} = \sqrt{\frac{d_{\mathrm{c}}^2 + d_{\mathrm{c}}d_{\mathrm{w}} + d_{\mathrm{w}}^2}{12}}$$

We used the equivalent radius to estimate the cross-sectional area of the muscle bundle, which was between 0.045 and 0.09 mm^2. Intact bundles were then mounted at the valve and the ventricular region by clips between either a force transducer or a voltage controlled motor positioner within a muscle measurement suite (Güth Scientific Instruments, Heidelberg, Germany). Stimulating pulse duration was 3.5 ms with an initial rate of 0.5 Hz. Increasing stimulating pulse duration beyond 5.0 ms significantly decreased force generation. The papillary bundle was continuously superfused with KH solution maintained at 34°C. Stimulation voltage and bundle length were adjusted until maximum force was reached. The fibre bundle was stimulated at 0.5 Hz for at least 30 min before executing the experimental protocol. Typically a muscle bundle will increase force after mounting due to washout of BDM and phosphorylation effects. After 30–45 min, the muscle bundle relaxed to a steady baseline. This increase in force with eventual relaxation seemed to correspond to phosphorylation states encountered by McClellan *et al.* (2001) after extraction of heart. A digital phosphor oscilloscope suite (Tektronix TDS 3014 with IEEE-488 communication module and Wavestar software, Oregon, USA) measured stimulation frequency, twitch force amplitude, averaged force amplitude within pre-set time windows, and continuously logged the data into the computer.

The experimental protocol consists of (1) increasing stimulation frequency from 0.5 Hz to 1.0 Hz, then continuing up to 8.0 Hz by 1.0 Hz increments (duration of 2 min or until a steady force value has been reached), (2) decreasing stimulation frequency to 0.5 Hz and superfusing with KH solution containing 5 μM of myristoylated autocamtide-2 related inhibitory peptide (AIP; Calbiochem, La Jolla, CA, USA) to inhibit CaMK2 or 1 μM of PKA inhibitor 14–22 amide (Calbiochem) for 25 min, and (3) repeating the 0.5 Hz to 8.0 Hz increase in stimulation frequency. The specificity of the CaMK2 inhibitor, AIP, was initially shown in pancreatic β-cells (Jones & Persaud, 1998) and has also been widely used in cardiac cells (Vinogradova *et al.* 2000; DeSantiago *et al.* 2002). In some experiments, the β-adrenergic receptor blocker, propranolol (1 μM), was perfused for 15 min before kinase inhibitor perfusion. In all experiments, active force describes the difference between the maximum and minimum force (passive tension) at a particular frequency.

Force–frequency with calcium measurements at room temperature

Right ventricular papillary muscle bundles were extracted and mounted in the same method as previously described. The same muscle measurement equipment suite provided all the optics and electronics needed for measuring intracellular calcium using Fura-2 dye. Measurements were collected through a different data acquisition suite (National Instruments A/D board and LabVIEW software) with the digital oscilloscope suite providing continuous monitoring. A mercury lamp and filter wheel provided alternating ultraviolet (UV) pulses of 340 nm and 380 nm at 250 Hz with pulse duration of 1.5 ms to illuminate the bundle. The combination of microscope, dichroic mirror, filter and photomultiplier tube (PMT) collected the Fura-2 fluorescence. A synchronized electronic integrator parsed and averaged the fluorescence from both 340 nm and 380 nm illuminations to the A/D system. The loading solution consisted of KH with 10 μM Fura-2 AM, 4.3 mg l^{-1} *N,N,N′,N′*-tetrakis(2-pyridylmethyl)ethylenediamine (TPEN), and 5.0 g l^{-1} cremophor. The KH to dimethyl sulfoxide (DMSO) volume ratio of the loading solution was 333 : 1. A loading duration of 1.5 h with 20 min of de-esterification gave signals of greater than 3-fold over background fluorescence. The ratio, R, of fluorescence from 340 nm excitation to fluorescence from 380 nm excitation was calculated after subtracting background fluorescence. Calcium concentration was calculated using the following equation (Grynkiewicz *et al.* 1985) with $K_{\mathrm{d,apparent}}$ equating to $K_{\mathrm{d}}\beta$ after subtracting background fluorescence:

$$[\mathrm{Ca}^{2+}] = K_{\mathrm{d}}\left(\frac{R - R_{\mathrm{min}}}{R_{\mathrm{max}} - R}\right)\beta$$

β is the ratio of the 380 nm signal at zero calcium *versus* the 380 nm signal at saturating calcium, 39.8 μM. An *in vitro* calibration utilizing 25 μM Fura-2 simulated *in vivo* conditions and produced the following values: $R_{\mathrm{min}} = 0.7$, $R_{\mathrm{max}} = 7.4$, and $K_{\mathrm{d,apparent}} = 3.29\ \mu$M. The experimental protocol was the same as described in the earlier section, except that stimulation frequency was increased only up to 3.0 Hz. A separate set of experiments with the same time sequence but without addition of AIP was conducted for both room temperature and 34°C experimental series. These time control experiments (data not shown) did not show any significant changes in FFR. A detailed method for the force–calcium data analyses is given in Supplementary material.

The rates of contraction and relaxation, $+\mathrm{d}F/\mathrm{d}t$ and $-\mathrm{d}F/\mathrm{d}t$, respectively, were approximated by force

measured at a prior sampling period subtracted by the current measurement divided by the sampling period (see the following equation).

$$\frac{dF}{dt} \approx \frac{F(t - \Delta T) - F(t)}{\Delta T}$$

$F(t)$ is the measured force at a particular time and ΔT is the sampling period, 1 ms. Averaging a three data point window for each single dF/dt calculation minimized the noise. In addition, we normalized the dF/dt to the cross-section area of muscle bundle to allow comparison between different experiments.

Back phosphorylation assay

Skinned myofibrils were isolated from ventricular muscle bundles incubated with or without either CaMK2 inhibitor or PKA inhibitor by a procedure modified from Pagani & Solaro (1981). Solutions contained 100 nM calyculin-A (a protein phosphatase-1 inhibitor) and protease inhibitors (complete-protease inhibitor cocktail tablet; Roche Applied Science, Indianapolis, IN, USA). Since CaMK2 phosphorylation is the enabling step for PKA phosphorylation, *in vitro* phosphorylation with exogenous PKA with γ-^{32}P will label all the unphosphorylated PKA sites to reflect the CaMK2 phosphorylation status. The *in vitro* phosphorylation condition consists of 75 μg myofilament protein incubated in the following solution for 30°C for 30 min: 200 μM ATP, 40 μCi [γ-^{32}P]ATP, 6250 units of the catalytic subunit of PKA (Calbiochem). Myofibrils were washed in phosphate buffer and solubilized in SDS-containing protein loading buffer. Equal amounts of protein (15 μg) were run on two 4–15% gradient gels for electrophoresis. One gel was stained with Coomassie blue, and the other gel was used for auto-radiography. After a short time exposure (usually 2–3 h), the bands representing TnI and MyBP-C were seen in the autoradiogram while 24–30 h exposure showed other bands including myosin light chain (MLC). The signal intensity of the TnI, MyBP-C and MLC bands were quantified by using Multi Analyst Software (Bio-Rad). The other gel was transferred to nitrocellulose with a Bio-Rad transblot apparatus. The filters were then incubated with a sarcomeric actin antibody 5C5 (1 : 5000 dilution) to verify equal loading, and this antibody was detected using the Pierce detection system (Pierce Biotechnology, Inc., Rockford, IL, USA). The actin band was also quantified using Multi Analyst Software (Bio-Rad). For statistical purposes, these two analyses (gel auto-radiography and Western blot) were performed 3 times with each sample. The gel loading for each sample was normalized with the actin band signal.

In order to determine whether BDM used in dissection of the fibres affects the phosphorylation status of these proteins, we dissected papillary fibres at two different conditions: one in the presence of BDM and the other in the presence of KH solution containing 100 μM calcium. Immediately after dissection, the fibres were snap-frozen in liquid nitrogen and stored at −80°C. A third set of fibres was dissected in the presence of BDM, mounted between two clips on the Güth instrument suite as described earlier, and stimulated at 0.5 Hz at 34°C for 30 min. These fibres were then snap-frozen and stored at −80°C. Myofibrillar proteins were then isolated, and a back-phosphorylation assay was conducted as described above. The data showed there was no significant change in the phosphorylation status of MyBP-C and TnI at the three different conditions of processing the fibres (data not shown).

Statistical analyses

All data are expressed as means ± S.E.M. Statistical analyses were done using either a Student's paired *t* test or a two-way ANOVA with Fisher's or Bonferroni/Dunn's *post hoc* test. $P < 0.05$ was regarded as statistically significant.

Results

Alterations of the calcium–force loop by increasing stimulation frequency and CaMK2 inhibition

At all stimulation frequencies, force relates to intracellular calcium concentration ($[Ca^{2+}]_i$) in a hysteresis loop fashion, and the inhibition of CaMK2 changes these hysteresis loops (Fig. 1*C*). Figure 1*A* clearly shows that the calcium concentration rises and falls ahead of force production and relaxation. The hysteresis loop is formed by plotting force *versus* calcium concentration (Fig. 1*B*). Identification of three specific points (A, B and C) on the loop and three segments transitioning between the points facilitate analyses and interpretations of the data. Point 'A' on the loop occurs after full relaxation from a previous contraction. The maximum calcium concentration occurs at points 'B' and the maximum force at point 'C'. Force initially rises concordantly with increasing $[Ca^{2+}]_i$ from point A to point B. Then, force continues to rise despite decreasing $[Ca^{2+}]_i$ in the B-to-C segment and finally, force falls concordantly with decreasing $[Ca^{2+}]_i$ in the C-to-A segment. Increasing stimulation frequency shifts the loop to higher $[Ca^{2+}]_i$ and increasing force development (Fig. 1*C*). In addition, Fig. 1*C* shows that inhibiting CaMK2 depresses point C and changes both the B-to-C and C-to-A segments. The force and calcium data were further analysed to determine the stage(s) of the contractile

cycle where the CaMK2 inhibition occurred and the possible mechanism of its action.

Effects of increasing stimulation frequency and CaMK2 inhibition at points A and B

At point 'A', increasing stimulation frequency increased diastolic $[Ca^{2+}]_i$ without significantly changing the diastolic force of the fibres in both untreated and CaMK2 inhibitor-treated conditions. The force–$[Ca^{2+}]_i$ gain (G) was calculated as described in Supplementary material. As seen in Fig. 2*A*, the normalized gain (NG) decreased with increasing frequency (control: 0.5 Hz NG = 1 *versus* 3 Hz NG = 0.521 ± 0.043, $n = 5$, $P < 0.0001$), and CaMK2 inhibition via 5 μM AIP did not alter this relationship (CaMK2 inhibition: 0.5 Hz NG = 0.981 ± 0.064 *versus* 3 Hz 0.524 ± 0.052, $n = 5$, $P < 0.0001$).

At point 'B', increasing stimulation frequency increased both active force and $[Ca^{2+}]_i$ transients while maintaining a similar change in force (defined as total force minus passive tension) to change in $[Ca^{2+}]_i$ ratio. Delta gain (ΔForce/$\Delta[Ca^{2+}]_i$) quantifies the myofilament's ability to generate force per unit of calcium and was calculated as described in Supplementary material. Increasing stimulation frequency caused no change in the normalized delta gain (NDG) in control fibres (0.5 Hz NDG = 0.843 ± 0.065 *versus* 3 Hz NDG = 0.759 ± 0.107, $n = 5$, $P = 0.505$). Inhibiting CaMK2 caused significant depression of NDG only at 0.5 Hz (from 0.843 ± 0.065 to 0.370 ± 0.119; $n = 5$, $P = 0.04$; Fig. 2*B*).

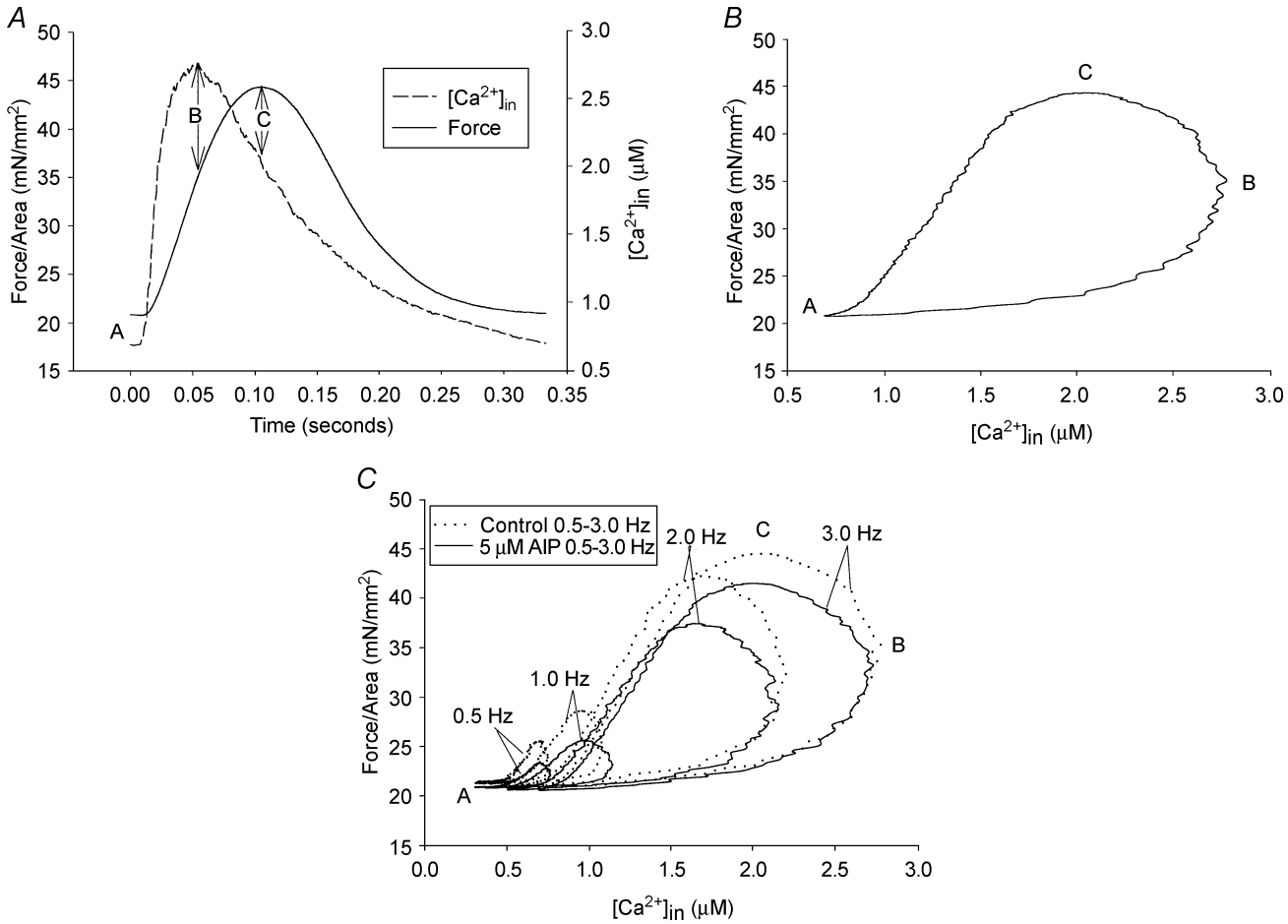

Figure 1. Force *versus* calcium relationship during a contraction cycle at room temperature
A, a representative graph showing calcium and force relationship with respect to time. 'A' is the resting (basal) point; 'B' is the maximum calcium point; 'C' is the maximum force point. *B*, an example of a force *versus* calcium hysteresis loop that can be divided into (1) calcium activation segment from A to B, (2) crossbridge feedback segment from B to C, and (3) relaxation segment from C to A. *C*, a representative graph showing inhibition of CaMK2 changes the calcium–force loop at room temperature.

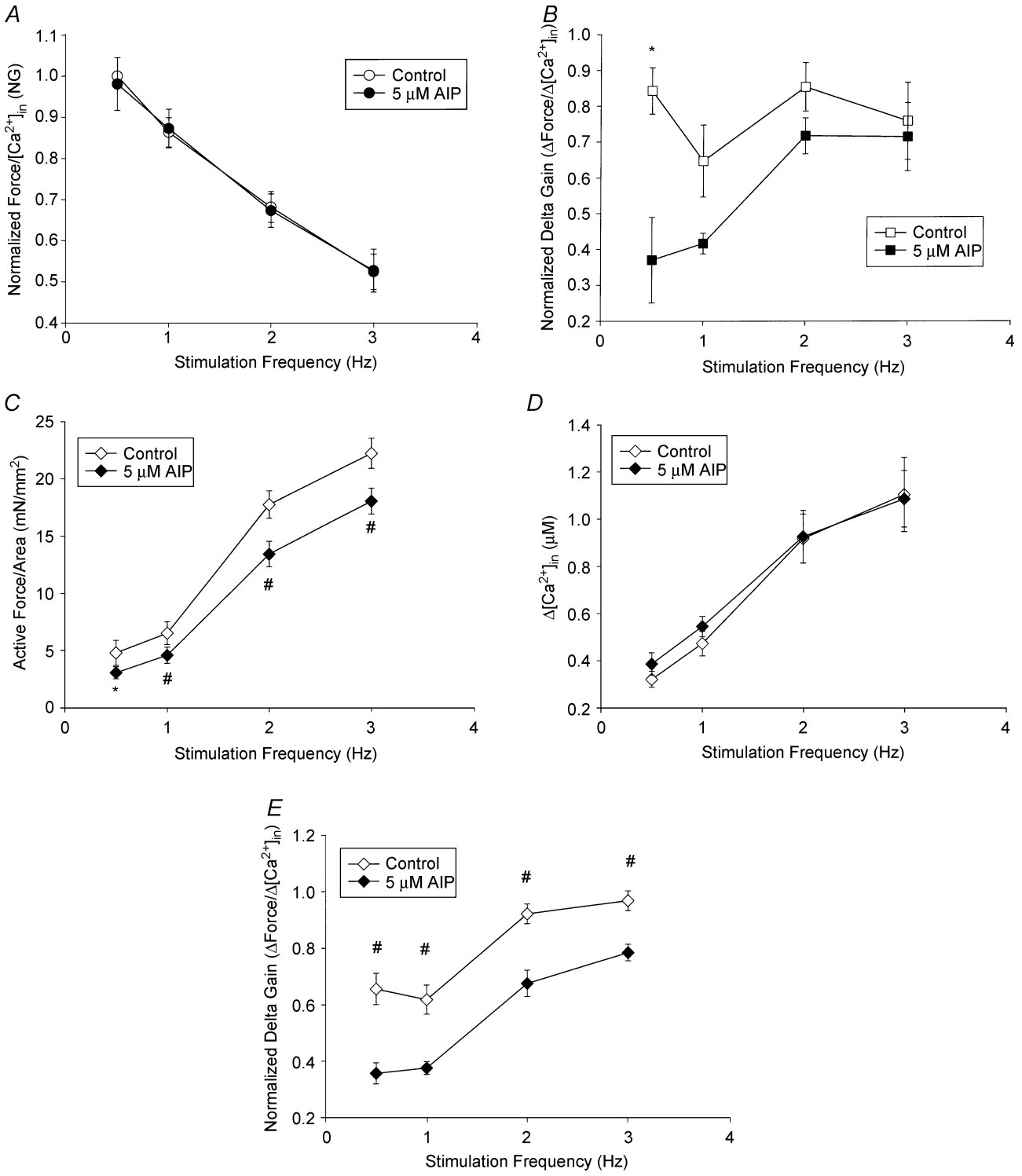

Figure 2. Calcium-force loop (at room temperature) analyses at different points
A, normalized force–$[Ca^{2+}]_i$ at the resting point, 'A', *versus* frequency was plotted for control and AIP-treated fibres. *B*, changes in active force/changes in $[Ca^{2+}]_i$ at the maximum calcium point, 'B', *versus* frequency was plotted for control and AIP-treated fibres; $^*P < 0.05$, paired *t* tests. *C*, active FFR at the 'C' point, $^*P < 0.05$, $\#P < 0.01$, paired *t* tests. *D*, changes in $[Ca^{2+}]_i$–frequency relationship at the 'C' state. *E*, changes in active force/changes in $[Ca^{2+}]_i$ at maximum force state 'C' for control and AIP-treated fibres. Data are means ± S.E.M.; $n = 5$. $\#P < 0.01$, paired *t* tests.

Table 1. Effects of CaMK2 Inhibition at the maximum force state 'C'

Frequency (Hz)	Mean active force difference (mN mm^{-2}) ($n = 6$)	P	Mean $\Delta[Ca^{2+}]_i$ difference (μM) ($n = 5$)	P	Mean NDG difference ($n = 5$)	P
0.5	− 1.72	0.03	+ 0.06	0.15	− 0.299	0.008
1.0	− 1.92	0.002	+ 0.07	0.06	− 0.242	0.001
2.0	− 4.30	0.001	+ 0.04	0.48	− 0.245	0.0003
3.0	− 4.17	0.008	− 0.02	0.55	− 0.183	0.010

Effects of increasing stimulation frequency and CaMK2 inhibition at point C

At point 'C', increasing stimulation frequency caused greater increases in the active force than in the calcium transients. Inhibiting CaMK2 depressed maximum active force across all frequencies without changing the increases in calcium transients (Fig. 2*C–E*). For control conditions, increasing stimulation frequency from 0.5 to 3.0 Hz caused active force to increase from 4.77 ± 1.09 to 22.05 ± 1.31 mN mm^{-2}, whereas CaMK2 inhibition resulted in changes from 3.04 ± 0.52 to 17.88 ± 1.12 mN mm^{-2} (Fig. 2*C* and Table 1). Interestingly, CaMK2 inhibition did not change $\Delta[Ca^{2+}]_i$ at all frequencies (Fig. 2*D* and Table 1). Thus, the depression of active force without changing $\Delta[Ca^{2+}]_i$ in the presence of the CaMK2 inhibitor lowered NDG across all frequencies (control values from 0.655 ± 0.056 to 0.961 ± 0.035; values for inhibitor treated condition, from 0.356 ± 0.037 to 0.778 ± 0.029, $n = 5$, $P < 0.0001$; Fig. 2*E* and Table 1). Since NDG quantifies changes in force per unit of calcium, these data have demonstrated that CaMK2 inhibition alters the myofilament activation processes.

Effects of increasing stimulation frequency and CaMK2 inhibition on the transitions between the three points

We also wanted to employ a method that objectively compared all three segments (A to B, B to C, and C to A) of the calcium–force loop. The derivations of three equations that are based on both phenomenological and empirical models are detailed in Supplementary material. Table 2 provides the summary of the fitted results for all the segment points. The equation is as follows:

$$\text{Force} = a[Ca^{2+}]_i e^{(a+b)[Ca^{2+}]_i} \quad (1)$$

It is described in the Supplementary material and fits well the calcium *versus* force values in the A-to-B segment with $R \geq 0.91$ for most cases (Fig. 3*A*). In this equation, the factors a and b could be indexes of all the calcium-dependent and cooperative activation processes. Data analyses show that factor a increases with increasing frequency, whereas factor b decreases (Table 2). Inhibiting CaMK2 did not change the fitted a and b values of this segment, suggesting that CaMK2 inhibition does not affect the A to B segment. The following equation described in Supplementary material fits the B-to-C segment well with $R \geq 0.94$ for most cases (Fig. 3*B*):

$$\text{Force} = G\frac{k^n}{k^n + [Ca^{2+}]_i^n} + \text{Offset} \quad (2)$$

G is the force gain factor, k is the $[Ca^{2+}]_i$ where 50% of active force occurs, n is the measure of cooperativity associated with calcium, and Offset is the force at maximum calcium, 'B'. Increasing stimulation frequency increases G_0, increases k, but decreases n. Inhibiting CaMK2 depresses G_0 across all stimulation frequencies, but did not significantly affect K or n (Table 2), indicating that the effect of CaMK2 inhibition occurs in the B-to-C segment. The following equation fits the C to A segment well with $R \approx 0.99$ for most of the cases (Fig. 3*C*).

$$\text{Force} = F_0\frac{[Ca^{2+}]_i^n}{k^n + [Ca^{2+}]_i^n} + \text{Offset} \quad (3)$$

where F_0 is the maximum active force; k and n are as described in eqn (2) and Offset is the force at point 'A'. Increasing stimulation frequency increases F_0, increases k (i.e. decreases calcium sensitivity), and decreases n. Inhibiting CaMK2 decreases F_0 at 1.0–3.0 Hz and decreases the cooperative factor (n) in a statistically significant manner for 2.0 Hz and 3.0 Hz (Table 2). These data suggest that CaMK2 inhibition also occurs in the C-to-A segment.

Effects of increasing stimulation frequency and CaMK2 inhibition on the rates of contraction and relaxation

Rates of force production were calculated as described in Methods. Both rates of contraction (maximum (max) $+dF/dt$) and relaxation (max $-dF/dt$) were increased

Table 2. Summary of fittings

Frequency (Hz)	*'a'*	*'a'* AIP	P	*'b'*	*'b'* AIP	*P*			
0.5, $n = 4$	67.97 ± 67.47	5.77 ± 3.80	0.41	$(4.0 \pm 1.69) \times 10^7$	$(2.4 \pm 0.93) \times 10^7$	0.19			
3.0, $n = 5$	6982.1 ± 3201.3	4914.8 ± 2100.9	0.49	$(3.7 \pm 1.04) \times 10^6$	$(4.0 \pm 1.2) \times 10^6$	0.39			
P for 0.5 *versus* 3.0	0.04**	0.04**	—	0.006**	0.004**	—			
	G_0	G_0 AIP	*P*	*K* (μM)	K AIP (μM)	*P*	*N*	*N* AIP	*P*
0.5, $n = 5$	3.77 ± 0.97	2.31 ± 0.52	0.03*	0.78 ± 0.06	0.79 ± 0.04	0.92	37.16 ± 4.92	38.83 ± 5.26	0.86
3.0, $n = 5$	23.36 ± 4.20	17.98 ± 3.02	0.01*	2.73 ± 0.35	2.58 ± 0.28	0.34	12.81 ± 2.66	14.44 ± 3.01	0.24
P for 0.5 *versus* 3.0	0.0002**	< 0.0001**	—	< 0.0001**	< 0.0001**	—	0.0001**	0.002**	—
	F_0	F_0 AIP	*P*	*K* (μM)	*K* AIP (μM)	*P*	*N*	*N* AIP	*P*
0.5, $n = 5$	5.55 ± 1.43	3.64 ± 0.73	0.06	0.95 ± 0.07	0.69 ± 0.04	0.07	17.61 ± 2.82	12.60 ± 1.03	0.07
1.0, $n = 5$	7.52 ± 1.22	5.61 ± 0.96	0.01*	0.78 ± 0.05	0.83 ± 0.05	0.01	12.24 ± 0.71	10.10 ± 0.84	0.08
3.0, $n = 5$	24.41 ± 2.21	17.67 ± 1.29	0.005*	1.29 ± 0.12	1.24 ± 0.10	0.39	8.55 ± 0.88	7.01 ± 0.49	0.05*
P for 0.5 *versus* 3.0	< 0.0001**	< 0.0001**	—	< 0.0001**	0.0002**	—	0.0009**	0.0003**	—

* and ** denote statistically significant difference.

significantly with increasing stimulation frequency (Table 3). CaMK2 inhibition reduced the max $+\mathrm{d}F/\mathrm{d}t$ at 0.5 Hz (control $+\mathrm{d}F/\mathrm{d}t$ 83.30 ± 9.73 *versus* AIP $+\mathrm{d}F/\mathrm{d}t$ 60.83 ± 7.24; $P = 0.04$; $n = 5$); however, the max $-\mathrm{d}F/\mathrm{d}t$ was not reduced significantly (-54.47 ± 5.88 *versus* -45.67 ± 5.03; $P = 0.214$; $n = 5$). At 3.0 Hz, both $+\mathrm{d}F/\mathrm{d}t$ and $-\mathrm{dF/dt}$ were depressed in the presence of CaMK2 inhibitor (Table 3).

Measurements of force–frequency at 34°C

To determine the effect of CaMK2 inhibition at near-physiological temperature, we performed force–frequency experiments at 34°C. In general, the results at 34°C showed a similar pattern of increasing FFR (Fig. 4*A*) as the results from room temperature. However, the maximum force at 34°C peaks at 6–7 Hz, whereas at room temperature it peaks at 3 Hz. As seen in Fig. 4*A*, increasing stimulation frequency increased normalized active force from 0.38 ± 0.026 to 0.95 ± 0.02 in the control condition. Inhibition of CaMK2 with 5 μM AIP depressed the normalized active force across all frequencies ($n = 5$, $P < 0.05$) with greatest depression at 6–7 Hz ($n = 5$, $P < 0.01$). Back phosphorylation experiments showed that CaMK2 inhibitor reduced the relative levels of phosphorylation of MyBP-C and TnI (see below). Hence, we investigated whether PKA inhibition, which would also decrease the phosphorylation of both MyBP-C and TnI, would reduce the force production similar to CaMK2 inhibition. Figure 4*B* shows that the normalized active force is depressed at all frequencies with PKA inhibition ($n = 3$, $P < 0.005$).

To further determine whether adrenergic stimulation (i.e. the potential release of catecholamines from the nerve endings of the papillary muscle preparations) contributed to the depression of force in the presence of CaMK2 inhibitor, force measurements were conducted in the presence of propranolol to block β receptors. Immediately following the propranolol treatment, CaMK2 inhibitor was also added to the suffusion solution and force was measured. Figure 4*C* shows that CaMK2 inhibition depresses the active force significantly ($n = 5$; $P < 0.05$), even after the propranolol treatment. These results indicate that the effects of CaMK2 inhibition are independent of any effects seen by the potential release of catecholamines during papillary fibre stimulation.

Phosphorylation of MyBP-C and TnI

Back phosphorylation assays were used to give an estimate of the available phosphorylated sites of the isolated protein. A representative autoradiogram of back phosphorylation of the myofibrillar proteins is shown in Fig. 5*A*. As expected, the relative levels of phosphorylation of both MyBP-C and TnI were increased in the presence of the PKA inhibitor, 14–22 amide (Fig. 5*A*, top panel). Interestingly, the increase of phosphorylation in both of these proteins was also found after CaMK2 inhibition (AIP-treated myofibrils). However, we did not find any

changes in MLC phosphorylation in these myofibrils (data not shown). For the purpose of quantification, another set of gels was analysed by Western blot using the sarcomeric actin antibody, as described in Methods. The bottom panel in Fig. 5*A* shows the relative amount of actin protein in each sample. The signal intensity of the actin band was taken as a loading control to quantify the MyBP-C and TnI signals. The data indicate that relative to control myofibrils, phosphorylation of MyBP-C and TnI is increased by approximately 30% and 20%, respectively, in the AIP-treated myofibrils, and by approximately 25% and 28% in the 14–22 amide-treated myofibrils (Fig. 5*B*). These increases in the signal intensity are statistically significant ($P < 0.0001$; $n = 3$, ANOVA with Bonferroni/Dunn's *post hoc* test).

Discussion

In this study, we have characterized the time-varying calcium–force relationship of cardiac muscle. Results provide the first evidence that increasing stimulation frequency caused increases in force production per unit change of calcium concentration and decreases in frequency-dependent calcium sensitivity during the relaxation phase. Furthermore, the data show CaMK2 inhibition that decreases both MyBP-C

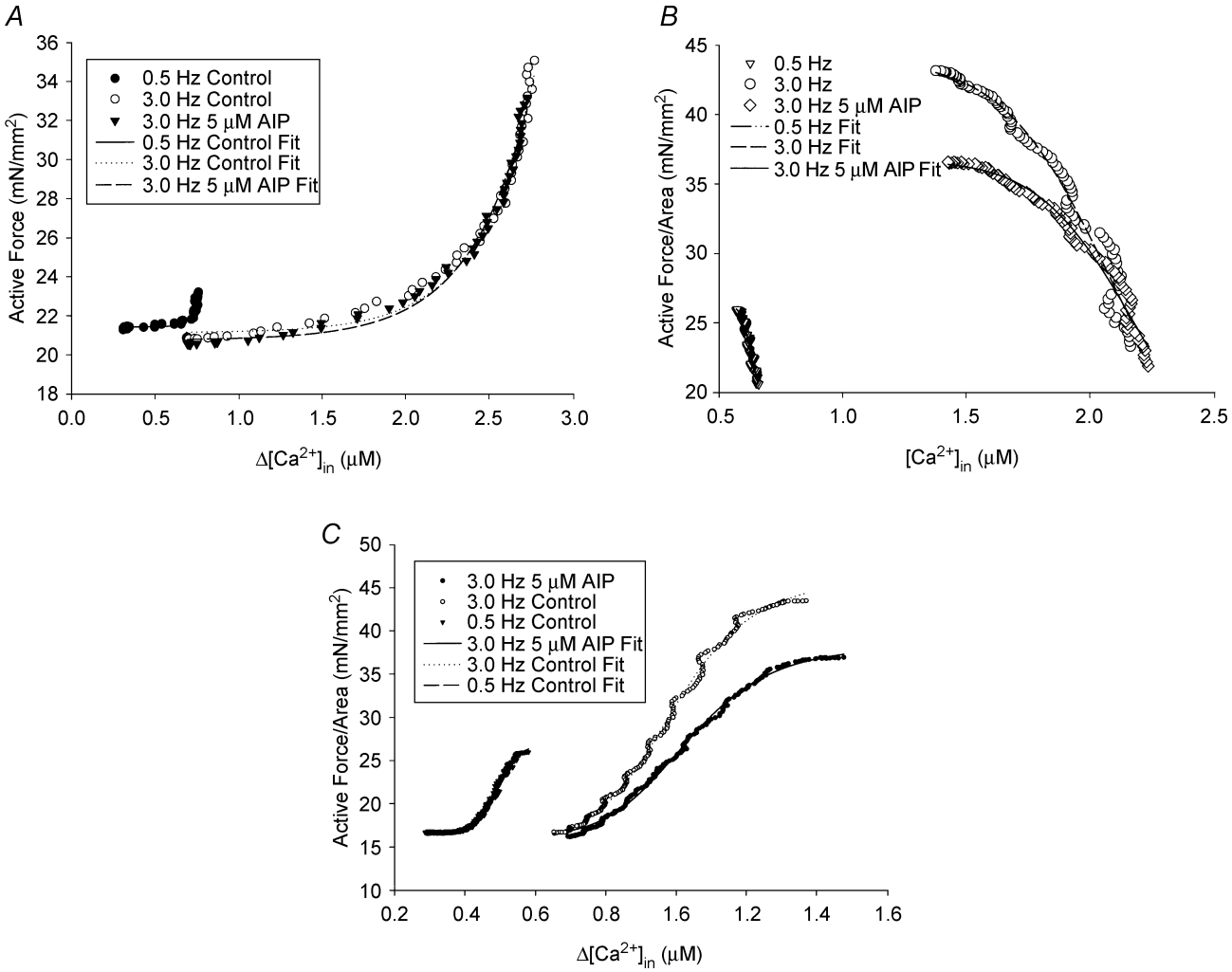

Figure 3. Segment analyses of calcium-force loop at room temperature
A, an example of the data points of active force *versus* changes in $[Ca^{2+}]_i$ for the A to B segment was fitted to eqn (1) for control and AIP-treated fibres. *B*, a representative graph of the data points of active force *versus* changes in $[Ca^{2+}]_i$ for the B to C segment was fitted to eqn (2) for control and AIP-treated fibres. *C*, an example of the data points of active force *versus* changes in $[Ca^{2+}]_i$ for C to A segment was fitted to eqn (3) for control and AIP-treated fibres.

Table 3. Maximum rates of force generation and relaxation

		Max +d*F*/d*t* (mN mm^{-2} s)			Max −d*F*/d*t* (mN mm^{-2} s)		
Frequency	*N*	Control	AIP	*P*	Control	AIP	*P*
0.5 Hz	5	83.30 ± 9.73	60.83 ± 7.24	0.04	−54.47 ± 5.88	−45.67 ± 5.03	0.214
3 Hz	5	375.43 ± 28.02	313.91 ± 27.85	0.001	−267.15 ± 14.09	−215.74 ± 12.49	0.001
P-value for 0.5 *versus* 3 Hz	—	< 0.0001	< 0.0001	—	< 0.0001	< 0.0001	—

N, number of experiments; +d*F*/d*t*, rate of force generation; −d*F*/d*t*, rate of relaxation.

and TnI phosphorylation levels reduces the maximum force through a crossbridge feedback mechanism.

Formation of the calcium–force loop

In the myofilament activation process, calcium binding to troponin C alters tropomyosin's position on actin from a blocked state ('off' state) to a closed state. This allows weak attachment of myosin heads to actin. The transition from the weakly bound crossbridges to the strongly bound state then moves tropomyosin to an open state ('on' state). This state facilitates further crossbridge binding, and the strongly bound crossbridges keep tropomyosin in the 'on' state (McKillop & Geeves, 1993; Geeves & Lehrer, 1994; Swartz *et al.* 1996; Vibert *et al.* 1997). Thus, for active force production, both calcium activation of the thin filament and positive feedback by strongly bound crossbridges are necessary. In addition, both of these mechanisms make significant contributions to each phase of the contractile cycle. Under this concept, one would expect increasing $[Ca^{2+}]_i$ to cause force initially to rise slowly in a linear fashion but make a transition to exponential growth. Concomitant increases in force and $[Ca^{2+}]_i$ in the A-to-B segment fits this well. Then as $[Ca^{2+}]_i$ starts to decrease, the crossbridge feedback seems to dominate as shown by continued rise of force despite decreasing $[Ca^{2+}]_i$ in the B-to-C segment. Eventually, the decrease in calcium overwhelms the crossbridge feedback effects on force development as seen in the C-to-A segment. This multistep process creates the hysteresis by requiring more $[Ca^{2+}]_i$ to start crossbridge binding but requiring less $[Ca^{2+}]_i$ to maintain the interaction due to crossbridge feedback. Direct measurement of crossbridge attachment using surface plasmon resonance showing a similar hysteresis loop supports this concept (Tong *et al.* 2001). Analyses of the active force production in the A-to-B and B-to-C segments show that the force generation is greater in the B-to-C segment (12.4, 17.8, 23.6 and 22.6% more force at 0.5, 1.0, 2.0 and 3.0 Hz, respectively), suggesting positive crossbridge feedback mechanisms provides the major part of force generation.

We have also derived three separate equations that describe the A-to-B, B-to-C and the C-to-A segments of the calcium–force loop. The data points fit the equations exceptionally well (Fig. 3*A*–*C*). However, the variables (*a*, *b*, *k* or *n*) within each equation that described the calcium and cooperative effects should be further verified, since both of these mechanisms contribute in each phase of the loop. Future studies using experimental perturbations in the specific activation mechanisms may be useful to understanding the contributions of calcium or cooperative effects to each phase of the loop, which would be helpful in quantifying these contributions using the variable presented in this study or modified variables in these equations.

Increasing stimulation frequency increases force production per change in calcium and decreases calcium sensitivity of myofilaments

Increasing stimulation frequency causes an increase in both active force and the transient $[Ca^{2+}]_i$ at the point of maximum force (point C). Further analyses demonstrate that the change in active force per change in calcium has increased as shown by increased normalized delta gain (NDG) with increasing frequency (Fig. 2*E*). These data corroborate well the findings of other groups demonstrating that increases in force are disproportionate to the increases in calcium transients, suggesting frequency-dependent 'sensitization' of myofilaments (Gao *et al.* 1998; Janssen *et al.* 2002). This clearly shows that the myofilament proteins must have changed their behaviour to make this possible. Interestingly, this increase in NDG occurs only at point C not at point B, suggesting the effects of change in myofilaments' characteristics occur mainly in the B-to-C segment but not at the A-to-B segment.

In addition, at point A, DG decreases with increasing frequency (Fig. 2*A*). The frequency-dependent increases in basal $[Ca^{2+}]_i$ at point A (from $0.387 \pm 0.054\ \mu$M at 0.5 Hz to $0.752 \pm 0.071\ \mu$M at 3 Hz; $n = 6$, $P < 0.0001$) has greater or near equal magnitude as the $\Delta[Ca^{2+}]_i$ at points B and C ($0.320 \pm 0.034\ \mu$M and $0.407 \pm 0.011\ \mu$M,

respectively). Furthermore the data analyses of the C-to-A segment showed that the increasing stimulation frequency increased k from $0.95 \pm 0.07\,\mu$M at 0.5 Hz to $1.29 \pm 0.12\,\mu$M at 3 Hz ($n = 5$, $P < 0.0001$) (Table 2 and Fig. 3*C*). These data demonstrate that increasing stimulation frequency causes a decrease in calcium sensitivity. Taken together, increasing stimulation frequency causes myofilament proteins to increase force production per change in calcium but raises the threshold for calcium activation.

Roles of MyBP-C and TnI phosphorylation

CaMK2 inhibition significantly depresses the NDG at all frequencies at point C (Fig. 2*E*). Concurrently, CaMK2 inhibition did not change $[Ca^{2+}]_i$ at either point C or B. These results demonstrate that CaMK2 inhibition decreases the frequency-dependent increase in force production per change of intracellular calcium. Furthermore, the CaMK2 inhibition effect occurs at the B-to-C segment without significantly impacting force production at point B. With crossbridge feedback most likely being the dominant mechanism in the B-to-C segment, we propose that phosphorylated MyBP-C exerts most of its effect during the crossbridge feedback mechanism. The depression of active force by the unphosphorylated C1C2 MyBP-C fragment (Kunst *et al.* 2000) and the increase in force after calcium-induced CaMK2 phosphorylation of MyBP-C (McClellan *et al.* 2001) further supports this finding. Kulikovskaya *et al.* (2003) have recently shown that extraction of MyBP-C from skinned fibres seems to produce a change in the

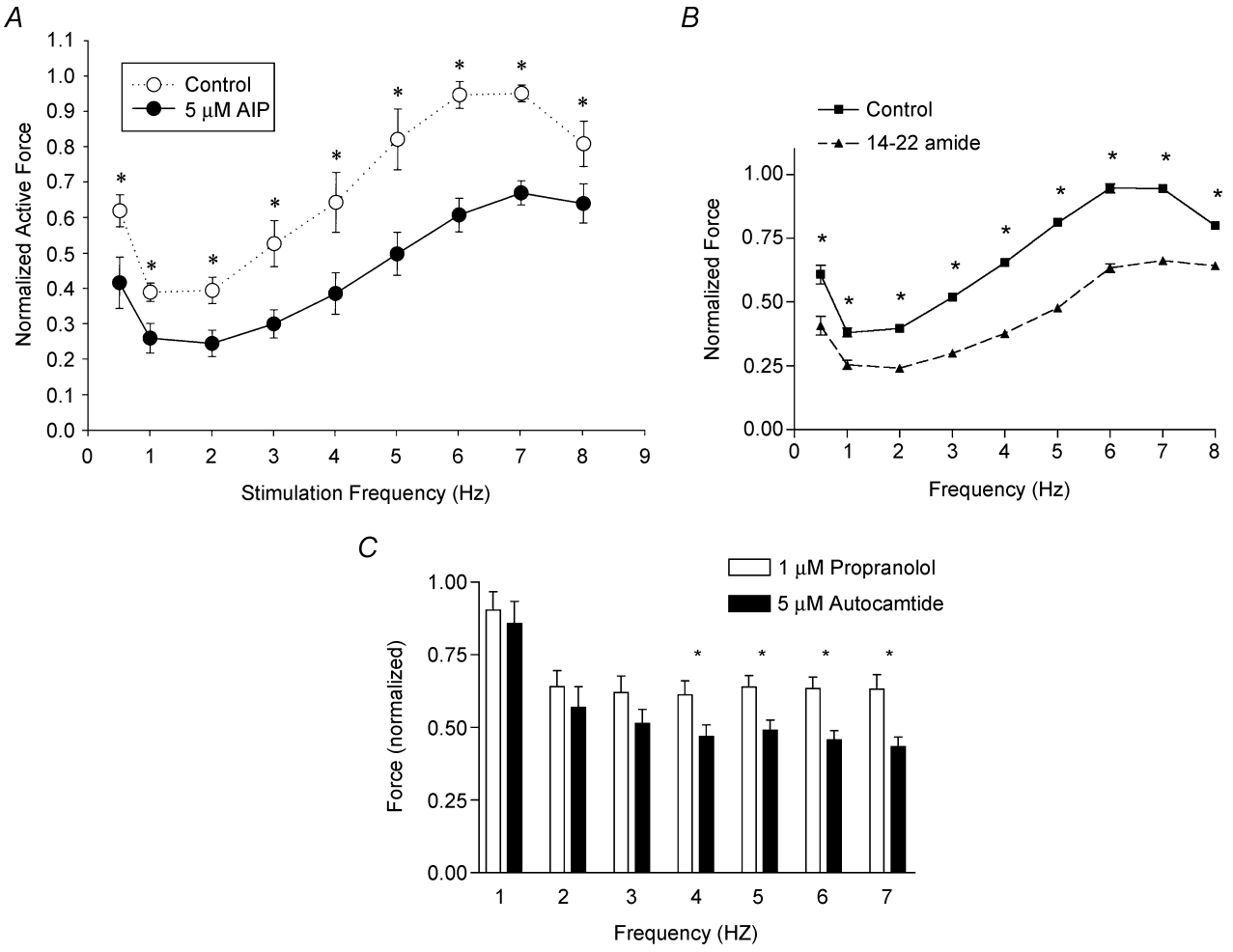

Figure 4. Normalized active force *versus* frequency of papillary fibre bundles before and after AIP (*A*) or 14–22 amide (*B*) treatment measured at 34°C

For *A*, data are means ± S.E.M.; $n = 5$. *$P < 0.05$, paired *t* tests. For *B*, data are means ± S.E.M.; $n = 3$. *$P < 0.005$, paired *t* tests. *C*, inhibition of force in the presence of CaMK2 inhibitor (AIP) after fibres were treated with propranolol. Data are means ± S.E.M.; $n = 5$, *$P < 0.05$, paired *t* tests.

orientation of myosin head and reduces F_{max}. In addition, MyBP-C knockout mouse hearts exhibit depressed contractile function with reduced Ca^{2+} sensitivity at the myofilament level (Harris *et al.* 2002). Regulatory myosin light chain (RMLC) is also phosphorylated in a frequency-dependent manner in the heart (Silver *et al.* 1986), which increases crossbridge cycling and speeds force development during stretch activation (Morano, 1999; Davis *et al.* 2001). However, the combination of a lack of changes in $[Ca^{2+}]_i$ transients and the lack of effect of CaMK2 inhibition on RMLC phosphorylation suggests that the effect of CaMK2 inhibition seen in this study is mainly due to MyBP-C and TnI phosphorylation.

To elucidate the role of MyBP-C phosphorylation by CaMK2 we used the CaMK2-specific inhibitor, AIP. This inhibitor peptide has been shown to specifically inhibit CaMK2 activity in previous studies (Jones & Persaud, 1998; Vinogradova *et al.* 2000; DeSanti-ago *et al.* 2002). However, a decrease in the phosphorylation of MyBP-C caused a reduction in TnI phosphorylation in our study (Fig. 5), indicating that functional coordination may be occurring between these two proteins. Hence, our results do not rule out the possibility that TnI phosphorylation plays a role in the crossbridge feedback segment. Yet, the possibility of cross-reactivity of AIP with PKA cannot be ruled out. Specific transgenic mouse models with mutations at either the CaMK2 and/or PKA phosphorylation sites of MyBP-C and mutations at the PKA sites of TnI would address the isolated effects of phosphorylation of these two proteins. However, a transgenic study in which a subset of phosphorylation sites in MyBP-C were removed showed a compensatory increase of phosphorylation in the remaining endogenous MyBP-C as well as an increase in the PKA-mediated phosphorylation of both TnI and phospholamban (Yang *et al.* 2001). These data support our observation that the decrease of MyBP-C phosphorylation in the AIP-treated samples causes a decrease in TnI phosphorylation.

Our results also imply that TnI may be phosphorylated in a coordinated manner in response to CaMK2 phosphorylation of MyBP-C, and phosphorylation of TnI could be a balancing mechanism to support the faster relaxation rates needed in the FFR. PKA phosphorylation of TnI decreases the calcium sensitivity of TnC (Chandra *et al.* 1997; Abbott *et al.* 2000) with the net overall effect of decreased myofilament calcium sensitivity and increased rates of relaxation (Solaro *et al.* 1976; Zhang *et al.* 1995; Solaro & Rarick, 1998; Kentish *et al.* 2001). Thus, our data that show the frequency-dependent decrease in calcium sensitivity, as previously discussed and an increase in the relaxation rates (Table 3) without change in calcium transients can be attributed to TnI phosphorylation. This coordination mechanism apparently adjusts both the force generation and relaxation to support the FFR.

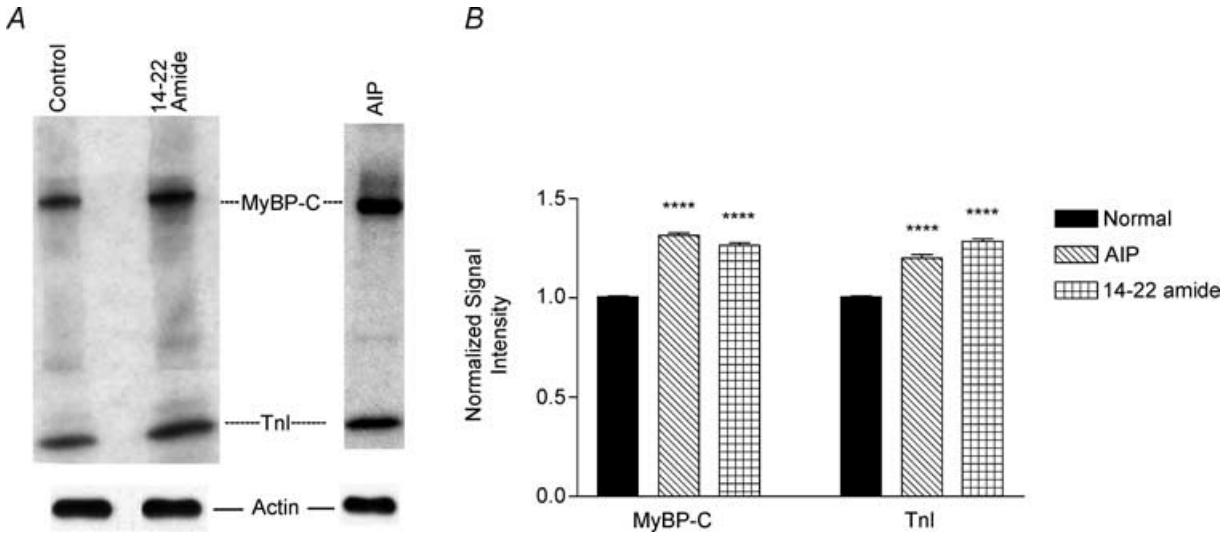

Figure 5. Back phosphorylation of myofibrillar proteins
A, top panel, representative autoradiogram of back phosphorylation of myofibrillar proteins isolated from papillary bundles incubated with CaMK2 inhibitor (AIP) or PKA inhibitor (14–22 amide). Bottom panel, representative data for the Western analysis of actin protein. *B*, quantitative analyses of relative levels of phosphorylation of MyBP-C and TnI resulting from 3 different back phosphorylation assays (*$P < 0.0001$; $n = 3$, ANOVA with Bonferroni/Dunn's *post hoc* test).

Yet, several studies indicate that TnI phosphorylation also plays an essential role in the rate of force production. Earlier studies by Strang *et al.* (1994) have shown that PKA phosphorylation of both MyBP-C and TnI increases the crossbridge cycling. Furthermore transgenic mouse hearts expressing constitutively phosphorylated TnI exhibit augmented force production and faster relaxation (Takimoto *et al.* 2004). Layland *et al.* (2004) have demonstrated that TnI phosphorylation may influence systolic performance in isolated heart preparations performing auxotonic contractions. Taken together, our data that show a decrease in the rates of contraction and relaxation with CaMK2 inhibitor, which reduced the relative levels of phosphorylation of both MyBP-C and TnI, indicate that phosphorylation effects of MyBP-C and TnI may interact with each other in a coordinated fashion to modulate contractility.

In summary, our data demonstrate that increasing stimulation frequency causes a change in the myofilament proteins' characteristics that increase force production per change in calcium but raises the threshold for calcium activation. In this process, phosphorylation of both MyBP-C and TnI contributes significantly in both the contraction and relaxation phases of the cardiac twitch cycle.

References

Abbott MB, Gaponenko V, Abusamhadneh E, Finley N, Li G, Dvoretsky A, Rance M, Solaro RJ & Rosevear PR (2000). Regulatory domain conformational exchange and linker region flexibility in cardiac troponin C bound to cardiac troponin I. *J Biol Chem* **275**, 20610–20617.

Alpert NR, Leavitt BJ, Ittleman FP, Hasenfuss G, Pieske B & Mulieri LA (1998). A mechanistic analysis of the force-frequency relation in non-failing and progressively failing human myocardium. *Basic Res Cardiol* **93**, 23–32.

Bluhm WF, Kranias EG, Dillmann WH & Meyer M (2000). Phospholamban: a major determinant of the cardiac force-frequency relationship. *Am J Physiol Heart Circ Physiol* **278**, H249–H255.

Bonne G, Carrier L, Richard P, Hainque B & Schwartz K (1998). Familial hypertrophic cardiomyopathy: from mutations to functional defects. *Circ Res* **83**, 580–593.

Braunwald E, Zipes DP & Libby P (2001). *Heart Disease*. W.B. Saunders Company, Philadelphia.

Brixius K, Reicke S & Schwinger RH (2002). Beneficial effects of the Ca^{2+} sensitizer levosimendan in human myocardium. *Am J Physiol Heart Circ Physiol* **282**, H131–H137.

Chandra M, Dong WJ, Pan BS, Cheung HC & Solaro RJ (1997). Effects of protein kinase A phosphorylation on signaling between cardiac troponin I and the N-terminal domain of cardiac troponin C. *Biochemistry* **36**, 13305–13311.

Craig R & Offer G (1976). The location of C-protein in rabbit skeletal muscle. *Proc R Soc Lond B Biol Sci* **192**, 451–461.

Davis JS, Hassanzadeh S, Winitsky S, Lin H, Satorius C, Vemuri R, Aletras AH, Wen H & Epstein ND (2001). The overall pattern of cardiac contraction depends on a spatial gradient of myosin regulatory light chain phosphorylation. *Cell* **107**, 631–641.

DeSantiago J, Maier LS & Bers DM (2002). Frequency-dependent acceleration of relaxation in the heart depends on CaMKII, but not phospholamban. *J Mol Cell Cardiol* **34**, 975–984.

Gao WD, Perez NG & Marban E (1998). Calcium cycling and contractile activation in intact mouse cardiac muscle. *J Physiol* **507**, 175–184.

Gautel M, Zuffardi O, Freiburg A & Labeit S (1995). Phosphorylation switches specific for the cardiac isoform of myosin binding protein-C: a modulator of cardiac contraction? *EMBO J* **14**, 1952–1960.

Geeves MA & Lehrer SS (1994). Dynamics of the muscle thin filament regulatory switch: the size of the cooperative unit. *Biophys J* **67**, 273–282.

Gruen M & Gautel M (1999). Mutations in beta-myosin S2 that cause familial hypertrophic cardiomyopathy (FHC) abolish the interaction with the regulatory domain of myosin-binding protein-C. *J Mol Biol* **286**, 933–949.

Gruen M, Prinz H & Gautel M (1999). cAPK-phosphorylation controls the interaction of the regulatory domain of cardiac myosin binding protein C with myosin-S2 in an on-off fashion. *FEBS Lett* **453**, 254–259.

Grynkiewicz G, Poenie M & Tsien RY (1985). A new generation of Ca^{2+} indicators with greatly improved fluorescence properties. *J Biol Chem* **260**, 3440–3450.

Hagemann D, Kuschel M, Kuramochi T, Zhu W, Cheng H & Xiao RP (2000). Frequency-encoding Thr17 phospholamban phosphorylation is independent of Ser16 phosphorylation in cardiac myocytes. *J Biol Chem* **275**, 22532–22536.

Harris SP, Bartley CR, Hacker TA, McDonald KS, Douglas PS, Greaser ML, Powers PA & Moss RL (2002). Hypertrophic cardiomyopathy in cardiac myosin binding protein-C knockout mice. *Circ Res* **90**, 594–601.

Hashimoto K, Perez NG, Kusuoka H, Baker DL, Periasamy M & Marban E (2000). Frequency-dependent changes in calcium cycling and contractile activation in SERCA2a transgenic mice. *Basic Res Cardiol* **95**, 144–151.

Heerdt PM, Holmes JW, Cai B, Barbone A, Madigan JD, Reiken S, Lee DL, Oz MC, Marks AR & Burkhoff D (2000). Chronic unloading by left ventricular assist device reverses contractile dysfunction and alters gene expression in end-stage heart failure. *Circulation* **102**, 2713–2719.

Hofmann PA, Hartzell HC & Moss RL (1991). Alterations in Ca^{2+} sensitive tension due to partial extraction of C-protein from rat skinned cardiac myocytes and rabbit skeletal muscle fibers. *J General Physiol* **97**, 1141–1163.

Janssen P, Stull L & Marban E (2002). Myofilament properties comprise the rate-limiting step for cardiac relaxation at body temperature in the rat. *Am J Physiol Heart Circ Physiol* **282**, H499–H507.

Jones PM & Persaud SJ (1998). Ca^{2+}-induced loss of Ca^{2+}/calmodulin-dependent protein kinase II activity in pancreatic beta-cells. *Am J Physiol* **274**, E708–E715.

Kentish JC, McCloskey DT, Layland J, Palmer S, Leiden JM, Martin AF & Solaro RJ (2001). Phosphorylation of troponin I by protein kinase A accelerates relaxation and crossbridge cycle kinetics in mouse ventricular muscle. *Circ Res* **88**, 1059–1065.

Kulikovskaya I, McClellan G, Levine R & Winegrad S (2003). Effect of extraction of myosin binding protein C on contractility of rat heart. *Am J Physiol Heart Circ Physiol* **285**, H857–H865.

Kunst G, Kress KR, Gruen M, Uttenweiler D, Gautel M & Fink RH (2000). Myosin binding protein C, a phosphorylation-dependent force regulator in muscle that controls the attachment of myosin heads by its interaction with myosin S2. *Circ Res* **86**, 51–58.

Layland J, Grieve DJ, Cave AC, Sparks E, Solaro RJ & Shah AM (2004). Essential role of troponin I in the positive inotropic response to isoprenaline in mouse hearts contracting auxotonically. *J Physiol* **556**, 835–847.

Lemaire S, Piot C, Leclercq F, Leuranguer V, Nargeot J & Richard S (1998). Heart rate as a determinant of L-type Ca^{2+} channel activity: mechanisms and implication in force-frequency relation. *Basic Res Cardiol* **93**, 51–59.

Li L, Satoh H, Ginsburg KS & Bers DM (1997). The effect of Ca^{2+}–calmodulin-dependent protein kinase II on cardiac excitation–contraction coupling in ferret ventricular myocytes. *J Physiol* **501**, 17–31.

McClellan G, Kulikovskaya I & Winegrad S (2001). Changes in cardiac contractility related to calcium-mediated changes in phosphorylation of myosin-binding protein C. *Biophys J* **81**, 1083–1092.

McKillop DF & Geeves MA (1993). Regulation of the interaction between actin and myosin subfragment 1: evidence for three states of the thin filament. *Biophys J* **65**, 693–701.

Miyamoto MI, Del Monte F, Schmidt U, DiSalvo TS, Kang ZB, Matsui T, Guerrero JL, Gwathmey JK, Rosenzweig A & Hajjar RJ (2000). Adenoviral gene transfer of SERCA2a improves left-ventricular function in aortic-banded rats in transition to heart failure. *Proc Natl Acad Sci U S A* **97**, 793–798.

Morano I (1999). Tuning the human heart molecular motors by myosin light chains. *J Mol Med* **77**, 544–555.

Munch G, Bolck B, Brixius K, Reuter H, Mehlhorn U, Bloch W & Schwinger RH (2000). SERCA2a activity correlates with the force-frequency relationship in human myocardium. *Am J Physiol Heart Circ Physiol* **278**, H1924–1932.

Offer G, Moos C & Starr R (1973). A new protein of the thick filaments of vertebrate skeletal myofibrils. Extractions, purification and characterization. *J Mol Biol* **74**, 653–676.

Pagani ED & Solaro RJ (1981). Methods for measuring functional properties of sarcoplamic reticulum and myofibrils in small samples of myocardium. *Meth Pharmacol* **5**, 49–61.

Silver PJ, Buja LM & Stull JT (1986). Frequency-dependent myosin light chain phosphorylation in isolated myocardium. *J Mol Cell Cardiol* **18**, 31–37.

Solaro RJ, Moir AJ & Perry SV (1976). Phosphorylation of troponin I and the inotropic effect of adrenaline in the perfused rabbit heart. *Nature* **262**, 615–617.

Solaro RJ & Rarick HM (1998). Troponin and tropomyosin: proteins that switch on and tune in the activity of cardiac myofilaments. *Circ Res* **83**, 471–480.

Spirito P, Seidman CE, McKenna WJ & Maron BJ (1997). The management of hypertrophic cardiomyopathy. *N Engl J Med* **336**, 775–785.

Strang KT, Sweitzer NK, Greaser ML & Moss RL (1994). β-adrenergic receptor stimulation increases unloaded shortening velocity of skinned single ventricular myocytes from rats. *Circ Res* **74**, 542–549.

Swartz DR, Moss RL & Greaser ML (1996). Calcium alone does not fully activate the thin filament for S1 binding to rigor myofibrils. *Biophys J* **71**, 1891–1904.

Takimoto E, Soergel DG, Janssen PML, Stull LB, Kass DA & Murphy AM (2004). Frequency- and afterload-dependent cardiac modulation in vivo by troponin I with constitutively active protein kinase A phosphorylation sites. *Circ Res* **94**, 496–504.

Tong CW, Kolemenski A, Lioubimov VA, Schuessler HA, Trache A, Granger HJ & Muthuchamy M (2001). Measurements of the cross-bridge attachment/detachment process within intact sarcomeres by surface plasmon resonance. *Biochemistry* **40**, 13915–13924.

Towbin JA & Bowles NE (2002). The failing heart. *Nature* **415**, 227–233.

Vibert P, Craig R & Lehman W (1997). Steric-model for activation of muscle thin filaments. *J Mol Biol* **266**, 8–14.

Vinogradova TM, Zhou YY, Bogdanov KY, Yang D, Kuschel M, Cheng H & Xiao RP (2000). Sinoatrial node pacemaker activity requires Ca^{2+}/calmodulin-dependent protein kinase II activation. *Circ Res* **87**, 760–767.

Weisberg A & Winegrad S (1996). Alteration of myosin cross bridges by phosphorylation of myosin-binding protein C in cardiac muscle. *Proc Natl Acad Sci U S A* **93**, 8999–9003.

Winegrad S (1999). Cardiac myosin binding protein C. *Circ Res* **84**, 1117–1126.

Winegrad S (2000). Myosin binding protein C, a potential regulator of cardiac contractility. *Circ Res* **86**, 6–7.

Yang Q, Hewett TE, Klevitsky R, Sanbe A, Wang X & Robbins J (2001). PKA-dependent phosphorylation of cardiac myosin binding protein C in transgenic mice. *Cardiovasc Res* **51**, 80–88.

Zhang R, Zhao J, Mandveno A & Potter JD (1995). Cardiac troponin I phosphorylation increases the rate of cardiac muscle relaxation. *Circ Res* **76**, 1028–1035.

Acknowledgements

We are grateful to Dr Michael Davis for his immense help in the LabVIEW programming. We also thank Dr Harris Granger for his critical reading of the manuscript. This work is supported by NIH grant HL-60758 to M.M.

Author's present address

C. W. Tong: Department of Internal Medicine, Duke University Medical Center, Durham, NC 27710, USA.

Supplementary material

The online version of this paper can be accessed at:
DOI: 10.1113/jphysiol.2004.062539
http://jp.physoc.org/cgi/content/full/jphysiol.2004.062539/DC1
and contains supplementary material entitled:
Roles of phosphorylation of myosin binding protein-C and troponin I in mouse cardiac muscle twitch dynamics.
This material can also be found at:
http://www.blackwellpublishing.com/products/journals/suppmat/tjp/tjp376/tjp376sm.htm